



Robust Stability Control of Inverted Pendulum Model for Bipedal Walking Robot

Ali Fawzi Abdul Kareem¹, Ahmed Abdul Hussein Ali^{2*}

Authors affiliations:

1) Mechanical Engineering
Department, University of
Baghdad, Baghdad-Iraq.
ali.fawzi.1989162@gmail.com

2*) Mechanical Engineering
Department, University of
Baghdad, Baghdad-Iraq.
ahmedrobot65@yahoo.com

Paper History:

Received: 7th Dec. 2019

Revised: 30th Dec. 2019

Accepted: 29th Jan. 2020

Abstract

This paper proposes robust control for three models of the linear inverted pendulum (one mass linear inverted pendulum model, two masses linear inverted pendulum model and three masses linear inverted pendulum model) which represents the upper, middle and lower body of a bipedal walking robot. The bipedal walking robot is built of light-weight and hard Aluminum sheets with 2 mm thickness. The minimum phase system and non-minimum phase system are studied and investigated for inverted pendulum models. The bipedal walking robot is programmed by Arduino microcontroller UNO. A MATLAB Simulink system is built to embrace the theoretical work. The results showed that one linear inverted pendulum is the worst performance, worst noise rejection and the worst set point tracking to the zero moment point. But two masses linear inverted pendulum models and three masses linear inverted pendulum model have a better performance, a better high-frequency noise rejection characteristic and better set-point tracking to the zero moment point.

Keywords: Robust Stability, Control of Inverted Pendulum, Robust Control of Bipedal Robot.

السيطرة القوية على استقرارية روبوت ثنائي الارجل عن طريق نموذج البندول المقلوب

علي فوزي عبدالكريم، أ.د. أحمد عبدالحسين علي

الخلاصة:

في هذا البحث، تم اقتراح ثلاثة اشكال من البندول المقلوب للسيطرة القوية على استقرارية الروبوت ثنائي الارجل (بندول مقلوب ذو كتلة واحدة، بندول مقلوب ذو كتلتين وبندول مقلوب ذو ثلاث كتل) حيث تشير الى الجزء العلوي، الجزء الوسط والجزء السفلي للروبوت. تم بناء الروبوت الثنائي الارجل من صفائح الالمنيوم المقوى وذو كتلة خفيفة بسمك 2ملم. تم دراسة نظام الطور ونظام اللا طور لنماذج البندول المقلوب. تم برجة الروبوت ثنائي الارجل بواسطة المتحكم اردوينو UNO. تم محاكاة جميع النتائج نظريا بواسطة الماتلاب. بينت النتائج ان البندول المقلوب ذو الكتلة الواحدة الأسوأ من بين الانواع الثلاثة من حيث السيطرة على الضوضاء وسحب الروبوت الى نقطة الاتزان المطلوبة. اما بالنسبة للبندول المقلوب ذو كتلتين وذو ثلاث كتل انهما افضل في رفض الضوضاء وسحب الروبوت لنقطة الاتزان المطلوبة.

1. Introduction

The humanoid or bipedal walking robot is one of the hot and fascinating objects of papers by engineers and scientists. Several kinds of humanoids are obtainable to depend on the functions, morphology, movement, and applications. All kinds have dynamic models and static models. Most of the researchers studied the problem of the stability of the humanoid. The humanoid is normally unstable, a considerable deal of overwork requires to spend on including that the control system backward the brains of the locomotion are robust and efficient [1]. When the humanoid's center of mass CoM is at all times inside

the region between the feet on the ground that called static balance. Dynamic balance takes place when the robot's CoM may be outside the region between the feet on the ground. Gait factors are step length, speed, the height of leg lift, maximal inclination angle trunk sideways and inclination angle of the trunk forward direction. There are several methods for dynamic balance, which are discussed in many types of research such as zero moment point ZMP, inverted pendulum, and genetic algorithm. The experiments of ZMP needs the knowledge of torque between the robot's ankle and foot or kinetic on the bipedal robot body [2]. This information can be found by using gyroscope sensors in the robot ankle or load cell sensors in the robot's



feet. With all dynamic forces and contact forces on the robot known, it is possible to calculate ZMP which is the dynamic equivalent to the static CoM [3]. They designed a foot-mounted ZMP sensor depends on the load cell and ZMP data obtained from bipedal robot Mari-2 and Mari-1. Also, they compared the ZMP data and gait generation between human subjects and bipedal robots. Napoleon et al. proposed minimum phase system and non-minimum phase system by using two masses linear inverted pendulum model which represents the upper and lower body of the bipedal robot [4]. The design of the controller depends on the proposed model using optimal control by considering output is confirmed and described using simulation. Kemalettin and O. Kurt. suggested a generation algorithm based on moving support foot ZMP reference and the linear inverted pendulum model [5]. This type of generation possesses naturalness in that the zero moment point in the human walk doesn't stay constant, but it moves forward, bottom the supporting foot. K. H. et al. investigated an online learning framework to improve the robustness of the ZMP depends on the biped walking controller [6]. The objective is used for learning a feedforward compensative zero moment point CZMP trajectory from estimated ZMP errors during cyclic motions by using ZMP principles. Satoshi Ito et al. considered the balance control of a humanoid robot on the sloped ground or under a constant external force [7]. The proposed adaptive posture changes and realized a control method with the feedback of the GRF. Young-Dae Hong. proposed a stability control method for a dynamically modifiable bipedal walking robot using a CP tracking controller [8]. The key idea of this paper to discuss robust control of linear inverted pendulum model for a bipedal walking robot capable of walking for balancing.

2. Theoretical Part

a) Stability Theory

In this section, the principles of ZMP are studied. **Figure (1)** shows the phases of foot contact on the ground where the supporting point may be either bottom the heel (phase I), bottom the foot (phase II) and the toes (phase III). Also, the law of the ZMP displacement may be discussed as follows: in the beginning of phase I the ZMP bottom of the heel; at the end of phase I, it jumps to the foot center; at the end of phase II it's shifted bottom of the toes; at the end of the half-step the ZMP jumps under of the other foot which is now being in contact with the ground [9]. To calculate ZMP for a bipedal robot, forward kinematics hypothesis as follows [10]:

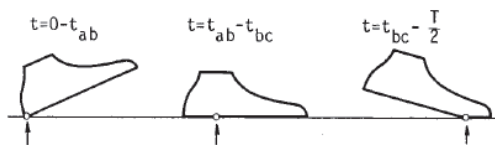


Figure 1: Phases of foot contact on the ground.

- The humanoid robot creates n links.

- All kinematic assumptions, like velocities, link orientation, and position of COM are estimated by kinematics principles.
- The ground is motionless and rigid.
- The foot can't slide above the floor surface.
- The joint is actuated.

Under these assumptions, the first step is to estimate m_{tot} of the bipedal robot and p_i :

$$m_{tot} = \sum_{i=1}^n m_i \quad (1)$$

And the distance from the origin to the CoM, p_{COM} and a graphical explanation are illustrated in **Figure (2)**.

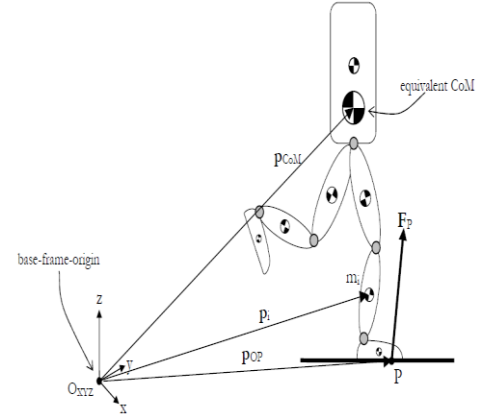


Figure 2: Schematic 3-D biped model and point p [11].

ZMP is generally used as balance control and standard estimation of the balance of bipedal walking robot. P is the linear momentum and H is the angular momentum concerning the base-frame-origin can be stated as:

$$P = \sum_{i=1}^n m_i \dot{p}_i \quad (2)$$

$$H = \sum_{i=1}^n \{p_i \times m_i \dot{p}_i + I_i \omega_i\} \quad (3)$$

Where ω_i and I_i are the angular velocity and the inertia tensor of the i -th link respectively w.r.t. the origin: For I_i the following equation holds:

$$I_i = R_i I_i R_i^T \quad (4)$$

Where R_i is the rotation matrix of i -th link w.r.t the origin connected to their links.

\dot{H} and \dot{P} are the rate of change of angular and linear momentums (being a moment and a force), respectively and can be derived as:

$$\dot{P} = \sum_{i=1}^n m_i \ddot{p}_i \quad (5)$$

$$\dot{H} = \sum_{i=1}^n (\dot{p}_i \times (m_i \dot{p}_i) + p_i \times (m_i \ddot{p}_i) + I_i \dot{\omega}_i + \omega_i \times (I_i \omega_i)) \quad (6)$$

Where $\dot{p}_i \times (m_i \dot{p}_i) = 0$ because \dot{p}_i and $(m_i \dot{p}_i)$ are parallel (note that $(m_i \dot{p}_i)$ is a scalar multiplication of (\dot{p}_i)). With this information the following holds [11]:

$$F_p = -F_A = \dot{P} - m_{tot} g \quad (7)$$

$$M_o = \dot{H} - p \times m_{tot} g \quad (8)$$

Where, as said earlier M_o and F_p are the moment and external forces that characterize how the floor is reacting to the humanoid w.r.t. the origin. F_A is the force that the humanoid is acting upon the ground. Also, the M_o is:

$$M_o = p_{op} \times F_p + M_p \quad (9)$$

Where p_{op} is the vector from the origin to point p and M_p is the moment at p. Because M_p is on the point p,



being either ZMP, its $M_p = [0 \ 0 \ M_z]$. Now, substitute eq. (7) and eq. (8) into eq. (9) resulting in:

$$M_p = \dot{H} - p_{CoM} \times m_{tot}g + (\dot{P} - m_{tot}g) \times p_{op} \quad (10)$$

From this, the distance from location of the ZMP to the origin $p_{zmp} = p_{op} = [x_{ZMP}, y_{ZMP}, z_{ZMP}]$ can be calculated [11]:

$$x_{ZMP} = \frac{m_{tot}g_z p_{CoMx} + z_{ZMP} \dot{P}_x - \dot{H}_y}{m_{tot}g_z + \dot{P}_z} \quad (11)$$

$$y_{ZMP} = \frac{m_{tot}g_z p_{CoMy} + z_{ZMP} \dot{P}_y - \dot{H}_x}{m_{tot}g_z + \dot{P}_z} \quad (12)$$

Where x_{ZMP} and y_{ZMP} are the distances from ZMP to the base-frame-origin about x-axis and y-axis respectively. Remind that z_{ZMP} is the height of the ground. When the plane is placed on the floor z_{ZMP} becomes zero.

Huang, et al. hypothesized that $z_{ZMP} = 0$, and described the following equation for deriving the ZMP [11]:

$$x_{ZMP} = \frac{\sum_{i=1}^n (m_i (p_{ix}(\ddot{p}_{iz} + g_z) - \dot{p}_{iz}(\dot{p}_{ix} + g_x)) - I_{iy}\omega_{iy})}{\sum_{i=1}^n m_i (\ddot{p}_{iz} + g_z)} \quad (13)$$

$$y_{ZMP} = \frac{\sum_{i=1}^n (m_i (p_{iy}(\ddot{p}_{iz} + g_z) - \dot{p}_{iz}(\dot{p}_{iy} + g_y)) - I_{ix}\omega_{ix})}{\sum_{i=1}^n m_i (\ddot{p}_{iz} + g_z)} \quad (14)$$

The only distinction from eq. (11), eq. (12) and eq. (13), eq. (14) is that the equations of the rate of angular momentum and linear momentum are derived in components.

Also, there is a final model to estimate ZMP and so-called Cart-Table model as shown in Figure (3). A model of a humanoid, which combined a moving cart on a massless table. Its positions (x,z) represents the CoM of the humanoid and the cart has mass m.

The τ around point p can be estimated as:

$$\tau = -mg(x_{CoM} - p) + m\ddot{x}_{CoM}z_{CoM} \quad (15)$$

In the eq. (15), g is the acceleration. Now, using the ZMP principles ($\tau = 0$) and thus $x_{ZMP} = p$, this results:

$$x_{ZMP} = p = x_{CoM} - \frac{\ddot{x}_{CoM}}{g} z_{CoM} \quad (16)$$

For the y-direction the derivation is similar, so:

$$y_{ZMP} = y_{CoM} - \frac{\ddot{y}_{CoM}}{g} z_{CoM} \quad (17)$$

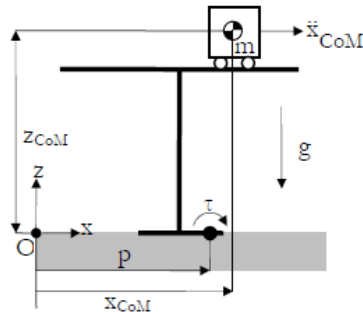


Figure 3: Cart-Table model [11].

b) Robust Control System

Systems are called robust when the systems have adequate variations in performance due to inaccuracies or model variations. A robust system appeared the required performance while the existence of considerable process uncertainty. The classical

feedback control system is the system structure that integrates the potential uncertainties as shown in Figure (4). This system consists of the sensor noise $N(s)$, the disturbance input $D(s)$, and a transfer function $G(s)$ with parameter changes and potentially unmodeled dynamics. The parameter changes and unmodeled dynamics may be significant, and for these systems, the robust is used to make a design that conserves the required performance. A system is said to robust when (1) it have low sensitivities, (2) is balance over the range of factor changes and (3) the performance sustained to meet the properties in the presence of a set changes in the system factors [12].

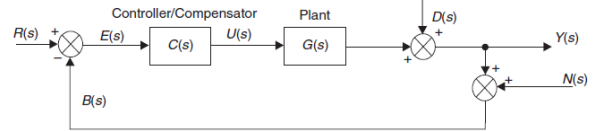


Figure 4: Classical feedback control system.

Robust systems are low sensitivity to effects that aren't significant in the design phase and analysis, for example, $N(s)$, $D(s)$, and unmodeled dynamics. The system must be capable to resist these eliminated changes when performing the functions for which it was designed.

$$\frac{Y}{D}(s) = S(s) = \frac{1}{1+G(s)C(s)} \quad (18)$$

And define a complementary sensitivity function

$$T(s) = 1 - S(s) = \frac{G(s)C(s)}{1+G(s)C(s)} \quad (19)$$

If $T(s) = 1$, there the system has both perfect noise acceptance and set-point tracking. However, the problem in the frequency domain, it may be considered that at low frequencies, complementary sensitivity $T(j\omega) \rightarrow 1$ (good set-point tracking) and the complementary sensitivity at high frequencies must be zero to give a good noise rejection. Robust stability can be explained in the frequency domain, using the Bode diagram. Also, it gives a minimum requirement in an environment where there is transfer function uncertainty. When the system has a robust performance, it should be able to minimize the error for the worst plant. For a robust system, $S(s)$ must be a small as possible. The frequency ω_n is a criterion of the boundary the region whose balance margin is important and between the frequencies regions in which the sensitivity is important. Thus, ω_n is properly to take into consideration the frequency of external disturbance and the extent of modeling error, the system expects to have a satisfactory value of robustness. The system is sensitive to changes in gain K and the performance of the system might be significant probably satisfactory for a variety of gain. The design of robust control systems depends on two factors: adjusting the controller's factor to make an "optimal" system performance and finding the structure of the controller. This design process is naturally achieved with "hypothesized complete knowledge" of the approach. In other words, the method is naturally characterized by a linear time-invariant continuous model [13]. To design a



controller, the structure of the controller must be chosen, such that the system's response can meet the considerable performance standards. One possible purpose in the design of a robust control system is that the output should instantaneously and exactly reproduce its input. Furthermore, the system must be adequate on a Bode gain versus frequency diagram with a 0-dB gain of zero phase shift and infinite bandwidth. In practice, this isn't sustained, since every system will contain capacitive and inductive type components that conserve energy in some form. These interconnections and elements with energy-dissipative components produce the system's dynamic response characteristics. Hence, the systems show some inputs aren't reproduced at all while the other inputs almost exactly, considering that the system bandwidth is less than infinite. Setting the design of robust systems in frequency-domain terms, a proper compensator $Gc(s)$ must be determined such that the closed-loop sensitivity is less than some tolerance value. But sensitivity reduction includes finding a suitable compensator such that the arbitrarily close to the minimal attainable sensitivity or the closed-loop sensitivity equals. Also, the gain margin problem is to determine a proper controller to obtain some prescribed gain margin. So, the gain margin maximization includes determining a proper compensator to consider the maximal obtainable gain margin. The objective of the robust control is to design a controller that regulates all plants lying within the specified domain of uncertainty. Considerably a controller is said to robustly balance the family of plants. Robust stability supplied a minimum necessity is an environment where there is a transfer function unconfirmed. For a control system to have a robust performance it must be able to minimize the error for the worst plant. The plant has neither zeros nor poles in the right half s plane is minimum phase transfer functions, whereas that has zeros and/or poles in the right half s plane is non-minimum phase transfer functions. A system with minimum phase transfer functions is called minimum phase systems, whereas the system with non-minimum phase transfer functions is called non-minimum phase systems. The non-minimum phase situations may arise in two different ways. One situation may arise in the case where a minor loop is unstable. The other is simply when a system includes elements or a non-minimum phase element. The response of the non-minimum-phase system is slow because of their incorrect behavior at the start of a response [13]. In the most practical control system, excessive phase lag should be carefully invalid. In designing a system if fast speed response is of primary importance, non-minimum phase components are not used as shown in **Figure (5)**.

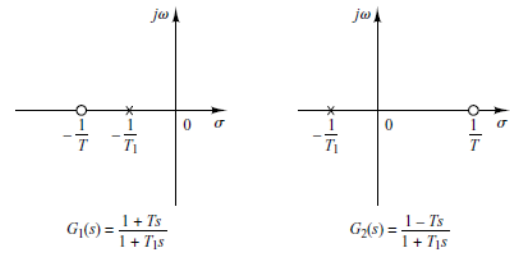


Figure 5: (a) Minimum phase system and (b) Non-minimum phase system.

c) Kinetic of Rigid Body system

Kinetic of Rigid Body

In this section, the kinetic of the linear inverted pendulum model is analyzed. **Figure (6)** shows one mass inverted pendulum model and the COM of the humanoid. The differential equation of the system is derived according to Newton's second law ($\sum M = Iu$). The one mass linear inverted pendulum, where it has a single input θ and single output ZMP p SISO system. And assumptions for the figure (small moment of inertia $I=0$) and for controlling the angle θ is small, where ($\sin \theta \approx \theta$ and $\cos \theta \approx 1$) [4]. Hence,

$$mg(p - l \sin \theta) + ml\ddot{\theta}(l) = 0 \quad (20)$$

$$p = [l \quad 0] \begin{bmatrix} \theta \\ \dot{\theta} \end{bmatrix} + \left[-\frac{l^2}{g} \right] u \quad (21)$$

The transfer function of the system is:

$$G(s) = \frac{gl - l^2s^2}{gs^2} \quad (22)$$

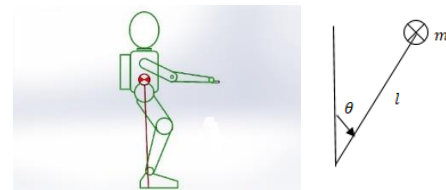


Figure 6: One mass inverted pendulum model.

Napoleon, et al., 2002. proposed ZMP feedback control using two masses linear inverted pendulum model which represents the upper and lower body of the bipedal robot as shown in **Figure (7)**. Two transfer functions are included: $\frac{p}{\theta_1}$. And $\frac{p}{\theta_2}$, (when considering input θ_1 , the input θ_2 is zero and vice versa is assumed). The input-output transfer function of the two masses inverted pendulum is [4]:

$$G(s) = \left[\frac{d_1s^2 + c_1}{s^2} \quad \frac{d_2s^2 + c_2}{s^2} \right] \quad (23)$$

For two DOF or double inverted pendulum the state space is shown:

$$\begin{pmatrix} A & B \\ C & D \end{pmatrix} = \begin{cases} \frac{d}{dt} \begin{bmatrix} \theta \\ \dot{\theta} \end{bmatrix} = \begin{bmatrix} 0 & 1 \\ 0 & 0 \end{bmatrix} \begin{bmatrix} \theta \\ \dot{\theta} \end{bmatrix} + \begin{bmatrix} 0 \\ l \end{bmatrix} u \\ p = [C_1 \quad 0] \begin{bmatrix} \theta \\ \dot{\theta} \end{bmatrix} + Du \end{cases} \quad (24)$$

Where

$$C_1 = \left[\frac{(m_1 + m_2)l_1 + m_2l_2}{m_1 + m_2} \quad \frac{m_2l_2}{m_1 + m_2} \right]$$

$$D_1 = \left[-\frac{m_1l_1^2 + m_2(l_1 + l_2)^2}{(m_1 + m_2)g} \quad -\frac{m_2(l_1 + l_2)l_2}{(m_1 + m_2)g} \right]$$

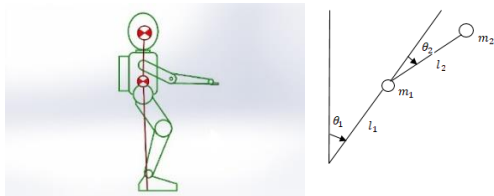


Figure 7: Two masses linear inverted pendulum of the bipedal walking robot.

In this work, three masses inverted pendulum model is investigated for improving the set-point tracking and noise rejection for the bipedal robot as shown in **Figure (8)**. Also, the transfer function of the three masses inverted pendulum model proposed in this work is similar to the two masses inverted pendulum model as shown in **eq. (23)** and **eq. (24)**. The difference between the transfer functions of two masses linear inverted pendulum model and three masses linear inverted pendulum model in the matrices C_1 and D_1 . Three transfer functions are included: $\frac{p}{\theta_1}$, $\frac{p}{\theta_2}$ and $\frac{p}{\theta_3}$ (when considering input θ_1 , the input θ_2 , and the input θ_3 are zero and vice versa is assumed).

Where

$$C_1 = \begin{bmatrix} \frac{m_1 l_1 + m_2 l_1 + m_2 l_2 + m_3 l_1 + m_3 l_2 + m_3 l_3}{m_1 + m_2 + m_3} & \frac{m_2 l_2 + m_3 l_2 + m_3 l_3}{m_1 + m_2 + m_3} \\ \frac{m_3 l_3}{m_1 + m_2 + m_3} & 0 \end{bmatrix}$$

$$D_1 = \begin{bmatrix} -\frac{m_1 l_1^2 + m_2 (l_1 + l_2)^2 + m_3 (l_1 + l_2 + l_3)^2}{(m_1 + m_2 + m_3)g} \\ -\frac{m_2 (l_1 + l_2) l_2 + m_3 (l_2 + l_3) (l_1 + l_2 + l_3)}{(m_1 + m_2 + m_3)g} \\ -\frac{m_3 (l_1 + l_2 + l_3) l_3}{(m_1 + m_2 + m_3)g} \end{bmatrix}$$

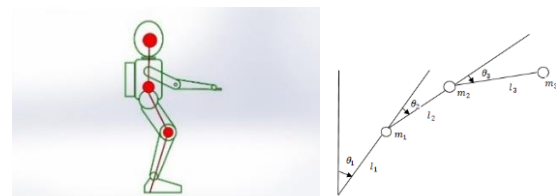


Figure 8: Three masses linear inverted pendulum model of the bipedal walking robot.

3. Experimental Part

The design of the humanoid robot involves both electronics and mechanical considerations equally. So, the design and fabrication of a bipedal robot are described. Also, all the devices that used for programming the bipedal robot by Arduino are illustrated in detailed. Analyzing, design and the making of the humanoid robot will be carried out through the following steps. A humanoid can be considered described as the kind of an autonomous system this can simulate human walking motion with maintaining postural stability during the walking. The design of a humanoid is very important for the accomplishable performance of the humanoid, especially the weight of the system hypothesizes physical limits. The servo motor type MG996R is used and will be arranged in the upper bracket and

connected with the lower bracket by screws as shown in **Figure (9)**. Two brackets are connected to create a link to the humanoid robot. The lower bracket is used to transmit the output of the servomotor and the servomotor will be fixed in the upper bracket. The bipedal robot can be broken into three blocks servo controller board, control unit and the servo used as an actuator. The PC sends the program to the Arduino microcontroller UNO bases on the movement required. The servo controller generates pulse width modulation PWM signal with period pulse width based on the instruction received thereby rotating the servos with angles and speed as required. The following experimental setup will show the components present in a humanoid robot. The initial design used 16 high-torque servomotors as shown in **Figure (10)** and resulted in a fast motion and quick reaction.



Figure 9: Black Aluminum sheets and high torque servo motor.

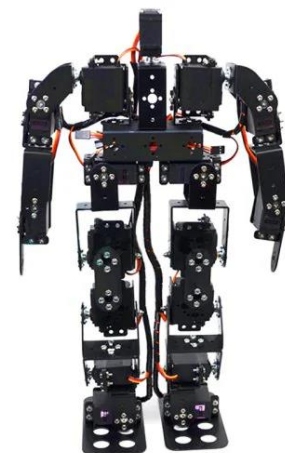


Figure 10: Bipedal walking robot.

For programming the bipedal walking robot, Arduino microcontroller is used and connected with



the PC. The main parts that need for programming the bipedal walking robot are:

- Arduino UNO,
- Battery LIPO 7.2V,
- Voltage regulator,
- Breadboard,
- 16-PWM channels servo driver Adafruit 96685.

The design concentrated primarily on the movement by using servos. The design for the walking distinct the servos with a parallel axis of rotation. But, this led to a significant problem through the lack of lateral balance control. The final design of the humanoid combined of two legs with five servos for each leg, and a microcontroller that is mounted on the head. The servos give a suitable amount of flexibility during the motion. The structure replaced with the head was used to house the controller and also the payload to the humanoid. Microcontroller, PCA 16 servo driver channel, battery, voltage regulator and bread are connected on the fiberglass board 2mm thickness. The main structure is built from the hard aluminum bracket of 2mm thickness. This provides enough strength, flexibility and gives the robot lightweight. The bracket is the manufacture of different sizes of sheets to connect with the servomotor in high precision [14]. The center of a mass of the humanoid is one of the necessary key parameters for stability. This is a parameter of weight distribution, the distance between the legs and the height of the robot. Angular motion is another significant factor in the counter-balance and balances the walking. The servomotors were placed in the knee, hip and ankle joints to get leg configuration similar to humans. The servos on the knee and hip have the same axis of rotation while the servomotor on the ankle joint moves the humanoid left and right. The ankle joint was chosen to rotate in this way to stabilize the humanoid's center of gravity from side to side while the knee and hip joints were designed to stabilize the humanoid about the backward and forward directions. **Figure (11)** shows the control panel of the bipedal robot.

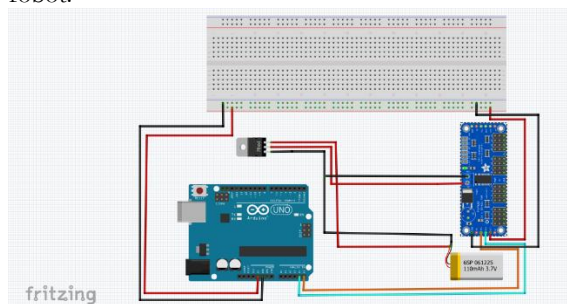


Figure 11: Control panel of the Robot.

The servomotors are connected with Arduino microcontroller UNO and are daisy-chained, so a serial port is considered to control the servomotors. The digital servos can act as actuators, electrical current data, and returning positions when being sent a suitable order sequence.

4. Robust Control Results

In this section, the effect of increasing the masses on the linear inverted pendulum model of robust stability control for the bipedal walking robot is discussed. To obtain the set-point tracking and noise rejection of robust stability control of the bipedal robot, a Bode diagram must be used. Napoleon, et al. showed that the one mass linear inverted pendulum model as shown in **Figure (6)** is a non-minimum phase system and improved that when proposed two masses linear inverted pendulum model. Hence, they showed that two masses linear inverted pendulum model is a minimum phase system [4]. First, the sensitivity of the one mass inverted pendulum is estimated according to **eq. (18)** and the complementary sensitivity must be calculated according to the **eq. (19)**. Simulation parameters of one mass linear inverted pendulum model of the bipedal robot are $m = 1.8kg$ and $l=28cm$. **Figure (12)** shows that the $T(j\omega)$ at low frequencies is between 0.01dB and climbs to 0.118 dB at high frequencies, hence the system tend to become the worst performance, worst set-point tracking to zero moment point reference and the worst noise rejection because the one mass linear inverted pendulum model is non-minimum phase system and has unstable zeros [4]. To minimize the estimation time during real-time application to maintain the stability and to simplify the design of the controllers it is generally used one mass model linear inverted pendulum model which represents the lower body of a humanoid. Thus, the stability control of the humanoid is conducted by moving the trunk of a humanoid so that the actual position of ZMP tracks the required position ZMP, while the upper body of the robot doesn't move too much. For improving the set-point tracking and noise rejection, two linear inverted pendulum model and three masses linear inverted pendulum model is proposed. For two masses linear inverted pendulum model as shown in **Figure (7)**, the mass of the lower body is represented by the center of mass and the mass of the upper body is represented at the head. Simulation parameters of two masses linear inverted pendulum model of the bipedal robot are $m_1 = 0.8kg$, $l_1=28cm$, $m_2 = 1kg$ and $l_2 = 10cm$. To analyze this system, it is essential to reduce the complexity of the expressions, as well as to resort to the computers for most of the tedious computations necessary in the analysis.

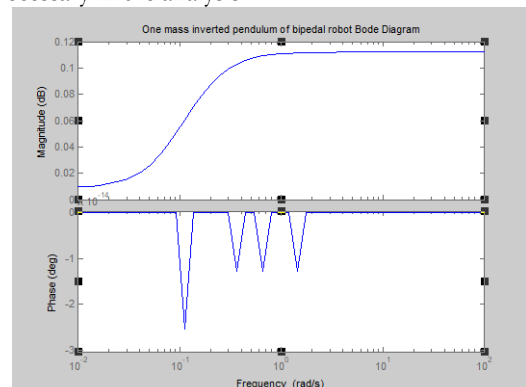


Figure 12: Complementary sensitivity of one mass inverted pendulum of bipedal robot Bode diagram.



The limitation in the performance of the robust stability control is happened because of the existence of unstable zero in the open-loop transfer function of the system. Thus, it needs to confirm that the new modeling of robust stability does not the system become bad noise rejection and set-point tracking. It can be examined by the analysis of zeros of the transfer function. However, since the new modeling consists of three inputs and one output, the concept of zero in the multi-input multi-output (MIMO) system is different from a single input single output SISO system. The zero of the system actually can be found by transforming systems to the Smith-McMillan form [4]. The system involves two inputs and one output. Two masses inverted pendulum is fast of responding because has stable zeros and tends to become a minimum phase system. In this work, set-point tracking to the reference ZMP is studied of the two pendulum model of the bipedal walking robot. **Figure (13)** shows the complementary sensitivity at low frequencies approximately 1.4dB and decreases to 0.1dB at high frequencies. The results showed that the system is approximately good noise rejection and good set-point tracking to the ZMP to the reference because the system has stable zeros and a minimum phase system. New modeling of three masses linear inverted pendulum model of a bipedal walking robot may have three inputs and one output, and these may be interrelated in a complicated manner. Two masses linear inverted pendulum model results showed that the system is the robust performance than one mass linear inverted pendulum model.

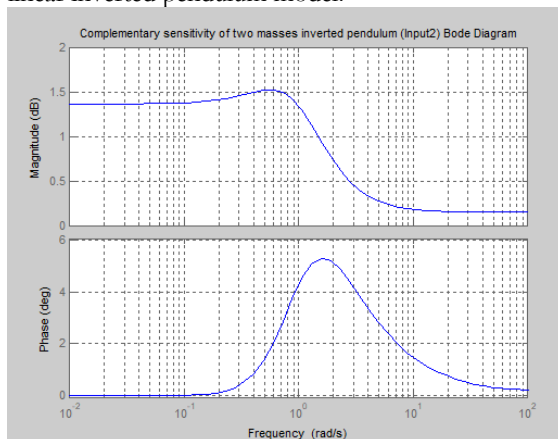


Figure 13: Complementary sensitivity of two masses inverted pendulum Bode diagram.

From the results, the reference and disturbance to the error of the system have closed-loop robustness and performance properties of the system. Thus, the system can make the reference quickly, it needs to give the sensitivity function $S(j\omega) \ll 1$ and the complementary sensitivity must be reduced from (1) to (0) at low frequencies and high frequencies respectively. Simulation parameters of three masses inverted pendulum as shown in **Figure (8)** of the bipedal robot are $m_1 = 0.4\text{kg}$, $l_1 = 14\text{cm}$, $m_2 = 0.4\text{kg}$, $l_2 = 14\text{cm}$, $m_3 = 1\text{kg}$ and $l_3 = 10\text{cm}$. **Figure (14)** showed that the complementary sensitivity at low frequencies approximately 1.38dB and falls to 0 dB at high frequencies. The results showed that the three masses inverted pendulum has better noise rejection

and better set-point tracking to the reference ZMP than two masses linear inverted pendulum model and one mass linear inverted pendulum model because the system has stable zeros and minimum phase system as shown in **Figure (14)**. Three masses linear inverted pendulum model results showed that the system is the robust performance than one mass linear inverted pendulum and two masses linear inverted pendulum model. Finally, if the system has unstable zeros, the system becomes the worst to set-point tracking to the zero moment point and the worst rejection. But, the system has stable zeros, the system has the better to set-point tracking to the zero moment point and the better noise rejection.

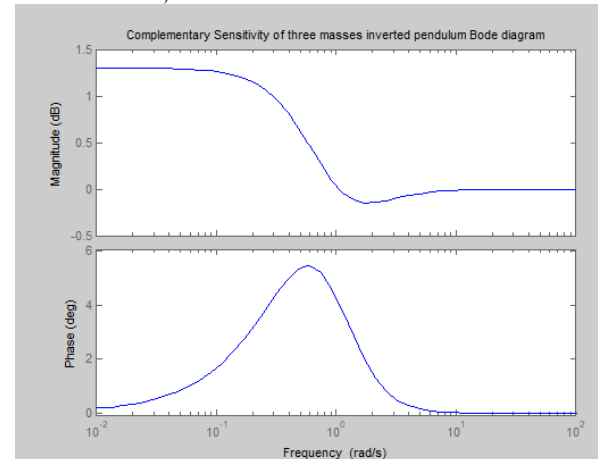


Figure 14. Complementary sensitivity of three masses inverted pendulum model.

5. Conclusions

This paper described the set-point tracking to the zero moment point and the noise rejection of the robust stability control for the bipedal walking robot. One mass linear inverted pendulum model has bad set-point tracking to the ZMP reference and bad noise rejection because the complementary sensitivity $T(j\omega)$ at low frequency approximated 0.01dB and climbs to 0.118 dB at high frequency due to the system has unstable zeros and non-minimum phase system. For improving the set-point tracking to the reference ZMP and noise rejection, two masses linear inverted pendulum and three masses linear inverted pendulum model are investigated. The complementary sensitivity of the two masses linear inverted pendulum model approximately (1.4 dB) at low frequency and falls to 0.1 dB at high frequency. So, the complementary sensitivity of three masses linear inverted pendulum model is (1.38 dB) at low frequencies and falls to (0 dB) at high frequency. The results showed that the three masses linear inverted pendulum model and two masses linear inverted pendulum model is the robust performance than one mass linear inverted pendulum. The proposed models have better set-point tracking to the zero moment point ZMP reference and better good noise rejection because it has stable zeros.

6. References

- [1] S. Warnakulasooriya, A. Bagheri, N. Sherburn and M. Shanmugavel, "Bipedal Walking Robot - A Developmental Design," International Symposium on



Robotics and Intelligent Sensors (IRIS), vol. 41, pp. 1016–1021, 2012.

[2] T. Bräunl, Embedded Robotics Springer, 2nd edition. 2006.

[3] K. Erbatur, A. Okazaki, K. Obiya, T. Takahashi and A. Kawamura, “A Study on the Zero Moment Point Measurement for Biped Walking Robots,” IEEE, pp. 431–436, 2002.

[4] Napoleon, S. Nakaura and M. Sampei, “Balance control analysis of humanoid robot based on ZMP feedback control,” IEEE, pp. 2437–2442, 2002.

[5] K. Erbatur and O. Kurt, “Humanoid Walking Robot Control with Natural ZMP References,” IEEE, pp.4100-4106, 2006.

[6] K. Hu, C. Ott and D. Lee, “Learning and Generalization of Compensative Zero-Moment Point Trajectory for Biped Walking,” IEEE, Vol. 32, pp.717-725, 2016.

[7] S. Ito, S. Nishio, Y. Fukumoto, K. Matsushita, and M. Sasaki, “Gravity Compensation and Feedback of Ground Reaction Forces for Biped Balance Control,” Hindawi, Vol. 2017, pp.1-16, 2017.

[8] Y. D. Hong, “Capture Point-Based Controller Using Real-Time Zero Moment Point Manipulation for Stable Bipedal Walking in Human Environment,” Sensors, Vol. 19, pp.1-18, 2019.

[9] M. Vukobratovic, B. Borovac and D. S. D. Stokic, Biped Locomotion Dynamics, Stability, Control and Application Springer, 1st edition. 1990.

[10] U. Huzaifa, C. Maguire, and A. LaViers, “Toward an Expressive Bipedal Robot: Variable Gait Synthesis and Validation in a Planar Model,” International Journal of Social Robotics, Vol. 2, pp.1-11, 2018.

[11] M.H.P. Dekker, “Zero-Moment Point Method for Stable Biped Walking,” Internship report, Eindhoven, Netherlands, pp. 1–50, 2009.

[12] R. C. Dorf and R. H. Bishop, Modern Control Systems, Prentice Hall, New Jersey eleventh ed. 2008.

[13] R. S. Burns, Advanced Control Engineering, 1st ed., Butterworth Heinemann, Oxford, 2001.

[14] A.F. Abdul Kareem and A.A. Ali, “Design of Optimal Stability Linear Inverted Pendulum Model

Control for Bipedal Robot,” REVISTA AUS, Vol. 26, pp.529-541, 2019.

7. Nomenclature

- F_p = External force, N.
 $G(s)$ = Transfer function.
 H = Angular momentum, kg.m²/s.
 I = Moment of inertia, kg.m².
 l = length of the pendulum, m.
 M = Moment, N.m.
 m = Mass of the robot, kg.
 $N(s)$ = Noise of the sensor.
 P = Linear momentum, kg.m/s.
 p = Zero moment point, m.
 p_i = distance of the center of link on the zero moment point, m.
 R = Rotation matrix.
 $R(s)$ = Input of the system.
 $S(s)$ = Sensitivity of the system.
 $T(s)$ = Complementary sensitivity.
 $u (\ddot{\theta})$ =Angular acceleration rad/s².

Greek Symbols

- | | |
|----------|------------------|
| τ | Torque |
| w | Angular velocity |
| θ | Angle |

Abbreviations

- | | |
|------|--------------------------------|
| CoM | Center of mass |
| CZMP | Compensative zero moment point |
| CP | Capture point |
| GRF | Ground reaction forces |
| MIMO | Multi input-multi output |
| PWM | Pulse width modulation |
| SISO | Single input-single output |
| ZMP | Zero moment point |